DFUB 98/22

ATMOSPHERIC NEUTRINOS AND NEUTRINO OSCILLATIONS

G.GIACOMELLI and M.SPURIO

Dipartimento di Fisica dell'Università di Bologna and INFN, Sezione di Bologna, 40127 Bologna, Italy
E-mail:giacomelli@bo.infn.it , spurio@bo.infn.it

Lecture at the Fifth School on Particle Astrophysics, Trieste 29 june-10 july 1998

Abstract

After some generalities on neutrino oscillations and on neutrinos, the recent experimental results presented by Soudan 2, MACRO and SuperKamiokande at the Neutrino'98 conference are summarized and discussed.

1. Introduction

Atmospheric neutrinos are produced in cosmic ray interactions in the upper atmosphere: a high energy primary cosmic ray, either proton or nucleus, interacts producing a large number of hadrons, in particular pions and kaons. These can decay giving rise to muons and muon neutrinos; also the muons decay yielding muon and electron neutrinos. In this simplified picture, the ratio of the numbers of muon to electron neutrinos is 2, $(N_{\nu_\mu}+N_{\overline{\nu}_\mu})/(N_{\nu_e}+N_{\overline{\nu}_e}) \simeq 2$, and $(N_\nu/N_{\overline{\nu}}) \simeq 1$, see Fig. 1. One may consider that these neutrinos are produced in a spherical surface at about few tens of km above ground, and that they proceed at high velocity towards the center of the earth.

The neutrino flux has been computed by a number of authors. At low energies $E_\nu \sim$ 1 GeV, the absolute numbers of predicted neutrinos differ by about 30%[2]; at higher energies, $E_\nu > 10$ GeV, the predictions are more reliable, with a systematic uncertainty of about 15%, that is about 1/2 of that at low energies[3]. However the predicted relative rates of ν_μ and ν_e and the shape of the zenith distribution have a considerably lower systematic

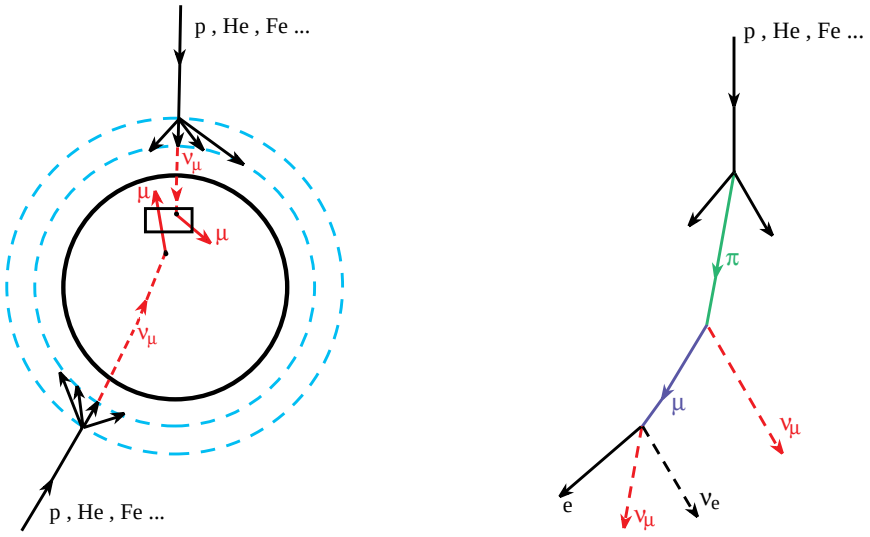

Figure 1: (a) Illustration of the production, travel and interactions of atmospheric muon neutrinos; (b) interaction of a primary cosmic ray, production of pions and their decays leading to the atmospheric ν_e, ν_μ.

error. Other sources of systematic uncertainties are due to the knowledge of the neutrino-nucleon cross sections and to the propagation of muons and electrons in different materials.

Since the 1980's several large underground detectors, mainly designed to search for proton decays, have studied atmospheric neutrinos. These detectors are located below 1-2 km of rock and they may detect neutrinos coming from all directions. Via charged current (CC) interaction the ν_μ gives rise to μ^- and thus to a track, the ν_e to e^- and thus to an electromagnetic shower. The produced hadronic system is not observed in most cases.

The detectors can be roughly classified as tracking calorimeters and as water Cherenkov detectors. The water Cherenkov detectors Kamiokande[4] and IMB[5] reported anomalies in the ratio of muon to electron neutrinos, while the tracking calorimeters NUSEX[6] and Frejus[7] did not find any deviation. Also the Baksan[8] scintillator detector did not see any deviation.

Later Soudan 2[9] and MACRO[10] reported deviations; in 1997 the neutrino anomaly was also reported by SuperKamiokande[11].

At the Session of June 5, 1998 at the Neutrino'98 Conference in Takayama, Japan, new, higher statistics data have been presented by the Soudan 2[12], MACRO[13] and SuperKamiokande[14] collaborations. The experiments con-

firmed the neutrino anomaly and opened a wide discussion on the subject.

The main purpose of this lecture is to review and discuss the presentations at the Neutrino'98 Conference. The SuperKamiokande results have been presented at this School by M. Koshiba[15]. Some results have been updated at the 1998 HEP Conference in Vancouver, Canada[16].

2. Neutrino oscillations

If neutrinos have non-zero masses one has to consider ν_e, ν_μ, ν_τ and their combinations. The ν_e, ν_μ, ν_τ are the appropriate particles to consider in weak decays, for example $\pi^+ \to \mu^+ + \nu_\mu$, and in charged current (CC) interactions which lead to their detection, e.g. $\nu_\mu + n \to \mu^- + p$; in technical terms one says that they are *weak flavour eigenstates*. Instead in the propagation in vacuum the appropriate particles are the *mass eigenstates* ν_1, ν_2, ν_3. The weak flavour eigenstates ν_l are linear combinations of the mass eigenstates ν_m:

$$\nu_l = \sum_{m=1}^{3} U_{lm}\ \nu_m \tag{1}$$

In the simplest case of only two neutrinos (ν_μ, ν_τ) which oscillate with two mass eigenstates (ν_2, ν_3) one may write

$$\begin{array}{l} \nu_\mu = \ \nu_2\ cos\ \theta_{\mu\tau} + \nu_3\ sin\ \theta_{\mu\tau} \\ \nu_\tau = -\nu_2\ sin\ \theta_{\mu\tau} + \nu_3\ cos\ \theta_{\mu\tau} \end{array} \tag{2}$$

where $\theta_{\mu\tau}$ is the mixing angle.

If the mixing angles are small one would have $\nu_e \sim \nu_1$, $\nu_\mu \sim \nu_2$, $\nu_\tau \sim \nu_3$; in this case one may speak of the mass of ν_e which is about equal to that of ν_1, etc. In the limit of zero masses the neutrinos become equal, and one does not need to introduce the ν_1, ν_2, ν_3. If the mixing angles are large, the situation is different and one has to consider well separated the eigenstates of flavour from those of mass. In particular it would be inappropriate to speak of mass for the weak eigenstates ν_e, ν_μ, ν_τ.

In the case of only two types of neutrinos, ν_μ and ν_τ, one may easily compute the following expression for the survival probability of a ν_μ beam:

$$P(\nu_\mu \to \nu_\mu) = 1 - sin^2 2\theta_{\mu\tau}\ sin^2(\frac{E_2 - E_1}{2}t) = 1 - sin^2 2\theta_{\mu\tau}\ sin^2(\frac{1.27\Delta m^2 \cdot L}{E_\nu}) \tag{3}$$

The probability for the initial ν_μ to have oscillated into a ν_τ is:

$$P(\nu_\mu \to \nu_\tau) = 1 - P(\nu_\mu \to \nu_\mu) = sin^2 2\theta_{\mu\tau}\ sin^2(\frac{1.27\Delta m^2 \cdot L}{E_\nu}) \qquad (4)$$

The mixing angle $\theta_{\mu\tau}$ and the mass difference $\Delta m^2 = \Delta m^2_{\nu_2\nu_3}$ may be determined from the variation of $P(\nu_\mu \to \nu_\mu)$ as a function of the zenith angle Θ, or the path L, or the energy E_ν or L/E_ν.

3. Early experiments

The ring imaging water Cherenkov detectors Kamiokande and IMB measured ν_μ and ν_e CC interactions and found that the ratio of muons to electrons was smaller than expected[1]. In the Kamiokande experiment, neutrino interactions were classified using the shape of the Cherenkov rings on the phototubes on the wall of the cylindrical water container, and through the recognition of muon decays. The results were expressed in terms of the ratio $R = R_{obs}/R_{MC}$ between $R_{obs} = (\frac{\nu_\mu}{\nu_e})_{obs}$ of measured CC interaction events and $R_{MC} = (\frac{\nu_\mu}{\nu_e})_{MC}$ from Monte Carlo simulations. The single ratio $(\nu_\mu)_{obs}/(\nu_\mu)_{MC}$, may be affected by large theoretical and systematic uncertainties; in the double ratio most systematic uncertainties cancel. The measured double ratios from Kamiokande[4] and IMB[5] are $R_{Kamioka} = 0.60 \pm 0.06_{stat+sys}$ and $R_{IMB} = 0.60 \pm 0.06_{stat} \pm 0.07_{sys}$, respectively. The NUSEX[6] and Frejus[7] tracking calorimeter detectors reported for contained and semicontained events $R_{obs} \sim R_{MC}$ within errors. The measured double ratios are: $R_{Nusex} = 1.0 \pm 0.3$, $R_{Frejus} = 0.99 \pm 0.13_{stat} \pm 0.08_{sys}$.

The Baksan scintillation telescope detected a sizable number of upthroughgoing muons arising from ν_μ interactions in the rock below the detector[8]. The average ν_μ energy for these events is considerably larger $(50-100\ GeV)$ than for the contained events measured by the other detectors. They did not find deviations from the predictions in the total number of events, but they find an anomalous angular distribution.

Later, the Soudan 2 tracking and shower calorimeter confirmed an anomaly in the ν_μ/ν_e ratio for contained events[9].

The MACRO[10] collaboration reported in 1995 a first measurement of upthroughgoing muons coming from ν_μ of $\overline{E}_\nu \sim\ 100\ GeV$ in which there was a deficit in the total number of observed upgoing muons, in particular

	Gold Data	Rock data	Background	Events	MC
Track	95	278	18.5 ± 6.1	76.9 ± 10.8	137.4
Showers	151	473	33.3 ± 12.8	116.3 ± 12.8	133.8

Table 1: Event summary for the Soudan 2 data. Track events are due to ν_μ while showers to ν_e. The MC predictions were obtained using the ν Bartol flux.

around the vertical, and also reported an anomalous zenith angle distribution. The deficit was confirmed at the 1996 and 1997 conferences[10].

At the 1997 conferences, the SuperKamiokande Collaboration confirmed the Kamiokande and IMB anomalies in the μ/e ratio for contained events[11].

4. Contained events and Soudan 2

The Soudan 2 data were presented at Neutrino'98 by E. Peterson[12]; improved data were presented at HEP'98 by H. Gallagher[12]. The Soudan 2 experiment uses a modular fine grained tracking and showering calorimeter of 963 t. It is located 2100 $m.w.e.$ underground in the Soudan Gold mine in Minnesota, USA. Its overall dimensions are $8m \times 16m \times 5m$. The *Central Detector* is made of 224 calorimetric modules of $1m \times 1m \times 2.5m$. The bulk of the mass consists of 1.6-mm-thick corrugated steel sheets which are interleaved with drift tubes. The detector is surrounded by an anticoincidence. This *Active Shield* detector covers the walls of the Soudan 2 cavern enclosing the Central Detector as hermetically as possible.

The neutrino contained events were selected by a combination of a two-stage software filter and a two-stage physicist scan. The software filter rejects non-contained events by requiring that *(i)* no part of the event is within 20 cm of the detector surface and *(ii)* no track is located or oriented in such a way that it could enter undetected in the calorimeter from a crack between modules. The last stage is the scan of real and simulated events. The MC simulated events were mixed with the real ones. All events were classified into one of three topologies: tracks (as due to ν_μ CC interactions); showers (ν_e CC interactions) and multiprongs (interactions of all neutrino flavors and NC). The multiprong events are not considered at present. Finally, events without any hits in the Active Shield detector are called *Gold Events*, while events with two or more hits in the shield are called *Rock Events*.

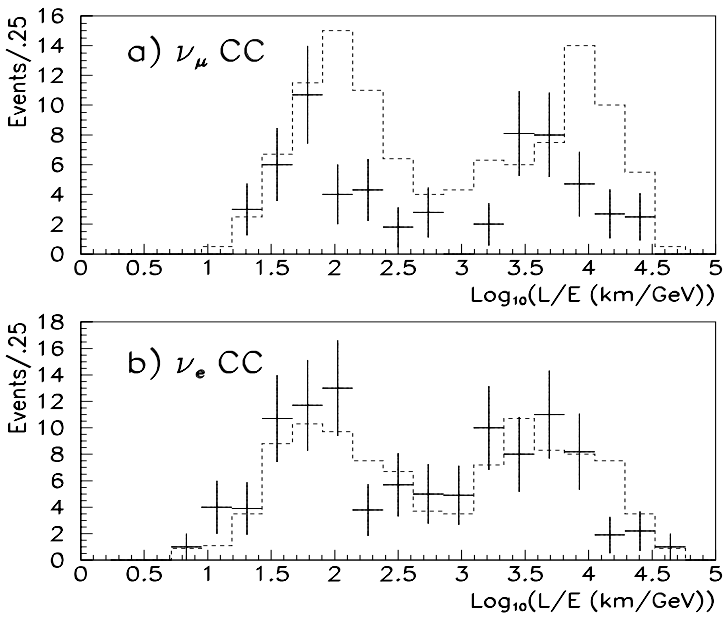

Figure 2: Soudan 2 (preliminary) results on the number of observed events as function of L/E: (a) for ν_μ and (b) ν_e. Only statistical errors are shown; the dashed lines are the MC predictions using the Bartol flux.

The data from a 3.89 $kt \cdot yr$ exposure are summarized in Table 1, together with the Monte Carlo predictions using the Bartol neutrino flux[17]. The Soudan 2 double ratio is $R = (N_\mu/N_e)_{data}/(N_\mu/N_e)_{MC} = 0.64 \pm 0.11^{+0.06}_{-0.05}$ which is consistent with muon neutrino oscillations.

For a smaller, high resolution sample, they are able to estimate the L/E for each event (Fig. 2), together with the MC predictions. Within limited statistics (after corrections, 60.8 ν_μ CC events and 106.4 ν_e CC events), the preliminary data are consistent with an anomaly in the muon data and not in the electron data. For this data set $R = 0.52 \pm 0.09_{stat}$. They add that $\Delta m^2 < 10^{-3}$ eV^2 appears unlikely.

5. Upward-going muons and MACRO

The MACRO data were presented at Neutrino'98 by F.Ronga[13]. The MACRO detector is located in Hall B of the Gran Sasso Laboratory, with a minimum rock overburden of 3150 hg/cm^2. It is a large rectangular box,

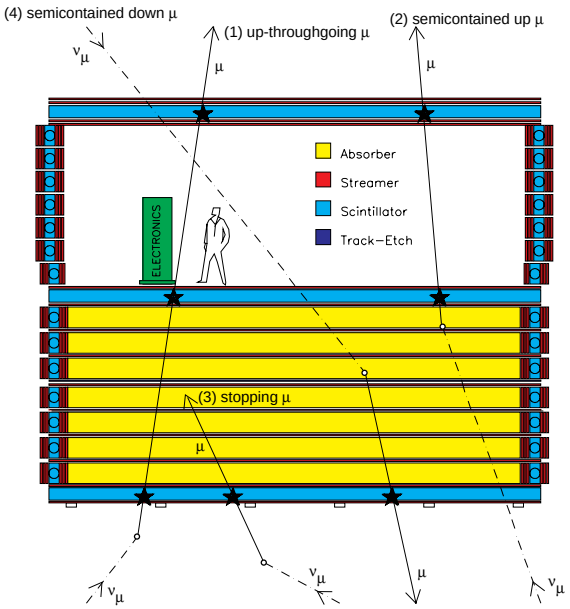

Figure 3: Sketch of different event topologies induced by ν_μ interactions in or around MACRO. The stars represent scintillator hits. The time-of-flight of the particle can be measured for *Up Semicontained* and *Up throughgoing* events.

76.6 m $\times$ 12 m $\times$ 9.3 m, divided longitudinally in six similar supermodules and vertically in a lower part (4.8 m high) and an upper part (4.5 m high). The detection elements are planes of streamer tubes for tracking and liquid scintillation counters for fast timing. The lower half of the detector is filled with trays of crushed rock absorbers alternating with streamer tube planes; the upper part is open and contains the electronics. There are 10 horizontal planes in the bottom half of the detector, and 4 planes on the top with wire and 27° stereo strip readouts. Six vertical planes of streamer tubes cover each side of the detector. The scintillator system consists of three layers of horizontal counters, and of one vertical layer along the sides of the detector. The time (position) resolution for muons in a scintillation counter is about 500 ps (11 cm). Fig. 3 shows a sketch of the three different topologies of neutrino events analyzed until now: up throughgoing muons, semicontained upgoing muons and up stopping muons+semicontained downgoing muons.

The *up throughgoing muons* come from ν_μ interactions in the rock below the detector, with $\overline{E}_\nu \sim 100\ GeV$. The muons ($E_\mu > 1\ GeV$) cross the whole detector. The time information provided by scintillation counters allows the

	Events detected	Predictions (Bartol neutrino flux)	
		No Oscillations	With oscillations
Up Through	451	$612 \pm 104_{th} \pm 37_{sys}$	$431 \pm 73_{th} \pm 26_{sys}$
Internal Up	85	$144 \pm 36_{th} \pm 14_{sys}$	$83 \pm 21_{th} \pm 8_{sys}$
In Down+Up Stop	120	$159 \pm 40_{th} \pm 16_{sys}$	$123 \pm 31_{th} \pm 12_{sys}$

Table 2: Event summary for the MACRO analysis. The predictions with oscillations are for maximum mixing and $\Delta m^2 = 0.0025\ eV^2$.

determination of the direction by the time-of-flight (T.o.F.) method. The data presented correspond to ~ 3.5 live years.

The *semicontained upgoing muons* come from ν_μ interactions inside the lower apparatus. Since two scintillation counters are intercepted, the T.o.F. is applied to identify the upward going muons. The average parent neutrino energy for these events is $\sim 4\ GeV$. If the atmospheric neutrino anomalies are the results of ν_μ oscillations with maximum mixing and Δm^2 between 10^{-3} and $10^{-2}\ eV^2$ one expects a reduction of about a factor of two in the flux of these events, without any distortion in the shape of the angular distribution.

The *up stopping muons* are due to external ν_μ interactions yielding upgoing muon tracks stopping in the detector; the *semicontained downgoing muons* are due to ν_μ induced downgoing tracks with vertex in the lower MACRO. The events are found by means of topological criteria; the lack of time information prevents to distinguish the two sub samples. An almost equal number of up stopping and semicontained downgoing events is expected, and the average neutrino energy for these events is around $4\ GeV$. In case of oscillations with the quoted parameters, a similar reduction in the flux of the up stopping events as the semicontained upgoing muons is expected. No reduction is instead expected for the semicontained downgoing events (from neutrinos having path lengths of $\sim 20\ km$).

The data were compared with Monte Carlo simulations. In the upgoing muon simulation the neutrino flux computed by the Bartol group[17] is used. The cross sections for the neutrino interactions have been calculated using the Morfin and Tung[18] parton distribution set S1. The propagation of muons to the detector has been done using the energy loss calculation by Lohmann *et al.*[19] in standard rock. The total systematic uncertainty from neutrino flux, cross section and muon propagation on the expected flux of muons is

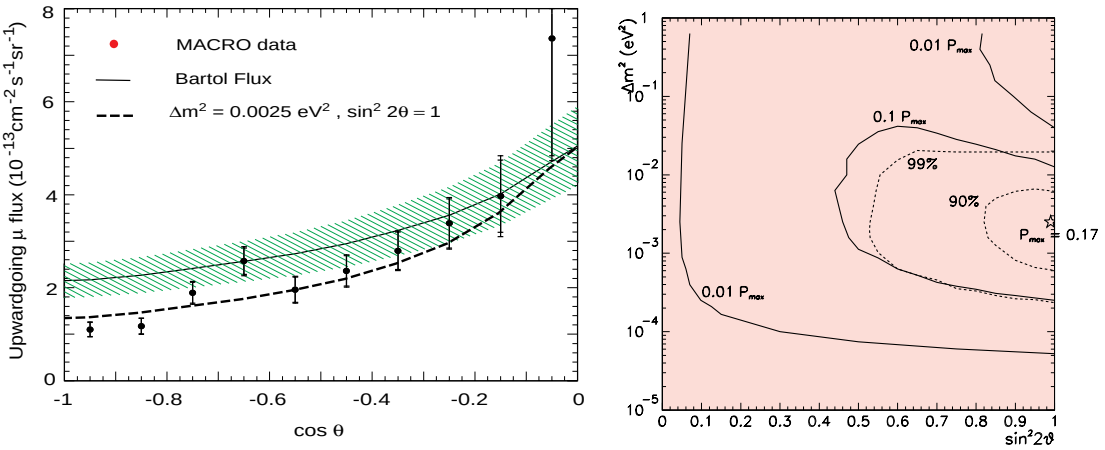

Figure 4: MACRO data. (a) Flux of the up throughgoing muons with $E_\mu > 1$ GeV vs. zenith angle Θ. The solid line is the expectation for no oscillations and the shaded region is a 17% scale uncertainty. The dashed line is the prediction for an oscillated flux with maximum mixing and $\Delta m^2 = 0.0025$ eV^2. (b) Probability contours for $\nu_\mu \to \nu_\tau$ oscillations. The dashed lines are 90% and 99% CL contours calculated according to[21]. The best probability is 17%; iso-probability contours are shown for 10% and 1% of this value (i.e. 1.7% and 0.17%).

$\sim$17%. Fig. 4a shows the zenith angle distribution of the measured flux of up throughgoing muons with energy greater than 1 GeV; the Monte Carlo expectation for no oscillations is shown as a solid line, and for a $\nu_\mu \to \nu_\tau$ oscillated flux with $\sin^2 2\theta = 1$ and $\Delta m^2 = 0.0025\ eV^2$ is shown by the dashed line. The systematic uncertainty on the up throughgoing muons flux is mainly a scale error that doesn't change the shape of the angular distribution. The ratio of the observed number of events to the expectation without oscillations is $0.74\ \pm 0.036_{stat}\ \pm 0.046_{sys}\ \pm 0.13_{theor}$.

The shape of the angular distribution of Fig. 4a has been tested with the hypothesis of no oscillation, giving a χ^2 of 26.1 for 8 degrees of freedom. Assuming $\nu_\mu \to \nu_\tau$ oscillations, the best χ^2 in the physical region of the oscillations parameters is 15.8 for $\Delta m^2 = 0.0025\ eV^2$ and $\sin^2 2\theta = 1$.

To test oscillation hypotheses, the independent probability for obtaining the number of events observed and the angular distribution for various parameter values have been calculated. The value of Δm^2 suggested from the shape of the angular distribution is similar to the value needed to obtain the

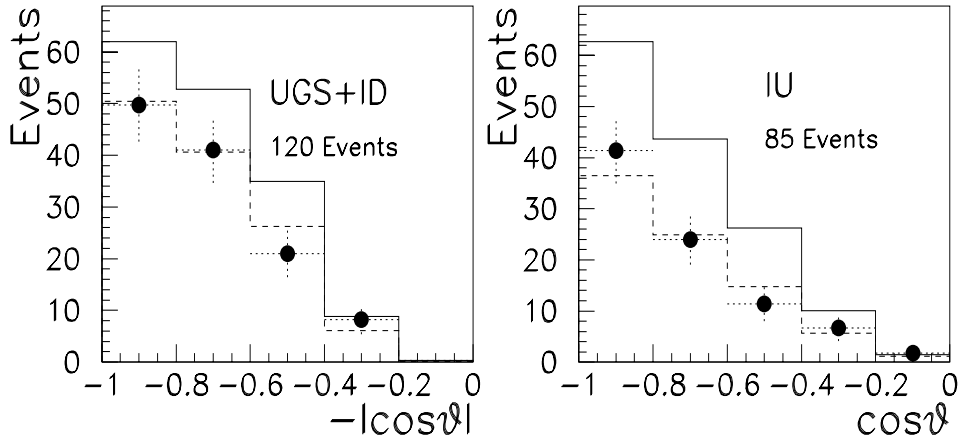

Figure 5: MACRO data. Measured and expected number of low energy events versus zenith angle; left: up stopping plus down semicontained; right: up semicontained. The solid lines are the predictions without oscillations; the dashed lines are the predictions assuming neutrino oscillations with the parameters suggested by the Up throughgoing sample.

observed reduction in the number of events in the hypothesis of maximum mixing. Fig. 4b shows probability contours for oscillation parameters using the combination of probability for the number of events and the χ^2 of the angular distribution. The maximum probability is 17%. The probability for no oscillations is 0.1%.

The MC simulation for the low energy data uses the Bartol neutrino flux and the neutrino low energy cross sections of ref.[20]. The number of events and the angular distributions are compared with the predictions in Table 2 and Fig. 5. The low energy data show a uniform deficit on the measured number of events over the whole angular distribution with respect to the predictions; there is good agreement with the predictions based on neutrino oscillations using the parameters obtained from the up throughgoing muon sample.

6. Results from SuperKamiokande and Kamiokande

SuperKamiokande is a large cylindrical water Cherenkov detector of 39 m diameter and 41 m height containing 50000 m^3 of water. The inner detector of 22500 m^3 is seen by 11146, 50-cm-diameter inner-facing phototubes. The

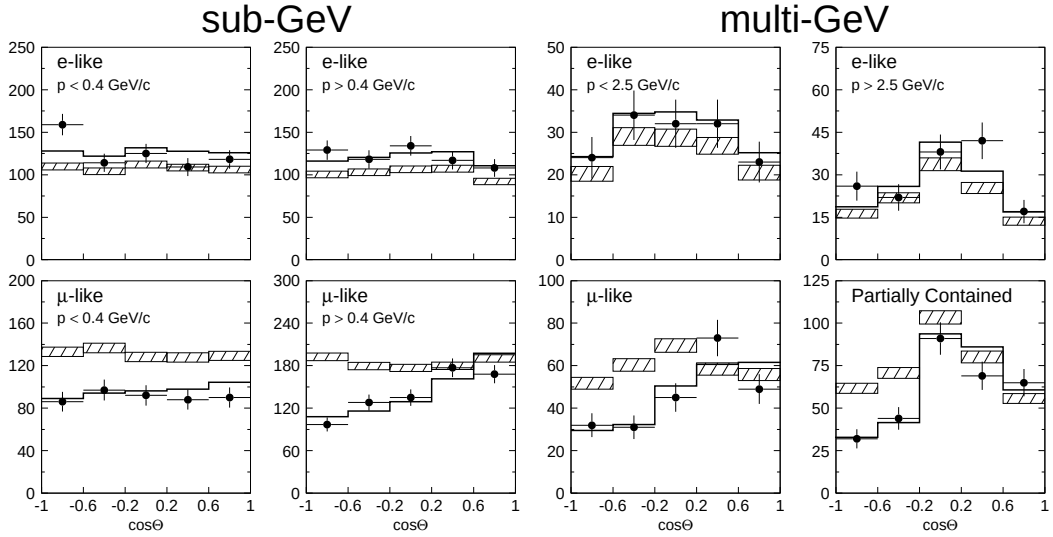

Figure 6: SuperKamiokande data. Zenith angle distributions of μ-like and e-like events for sub-GeV and multi-GeV data sets. Upward- going particles have $\cos\Theta < 0$. The hatched regions are the Monte Carlo expectation for no oscillations normalized to the detector live-time. The solid lines are the best-fit expectations for $\nu_\mu \to \nu_\tau$ oscillations with the overall flux normalization fitted as free parameter.

$2m$ thick outer layer of water acts as an anticoincidence and is seen by 1885 smaller outward-facing photomultipliers. The ultra pure water has a light attenuation of almost 100 m. The detector is located in the Kamioka mine, Japan, under 2700 $m.w.e.$. For more details see the lecture by M. Koshiba[15].

Because of the water index of reflection of 1.33, a relativistic charged particle (as the muon generated by a neutrino CC interaction) generates a 42^o forward cone of light. Instead electrons, being much lighter than muons, suffer electromagnetic showering and multiple scattering; therefore the ring of light is not so well defined as for the muons. The detector can distinguish single muons from single electrons with about 98% efficiency. Multiple ring events have been only partially used. The light intensity on the phototubes is a measure of the particle energy, and its direction is determined by the spatial and temporal pattern of phototube hits.

The data presented at Neutrino'98 correspond to 33 $kt \cdot yr$ of data. This exposure collected 4353 fully contained (FC) events and 301 partially contained (PC) events. The FC events were separated into "sub-GeV" (with $E_{vis} < 1.3\ GeV$) and "multi-GeV" ($E_{vis} > 1.33\ GeV$) samples; E_{vis} is de-

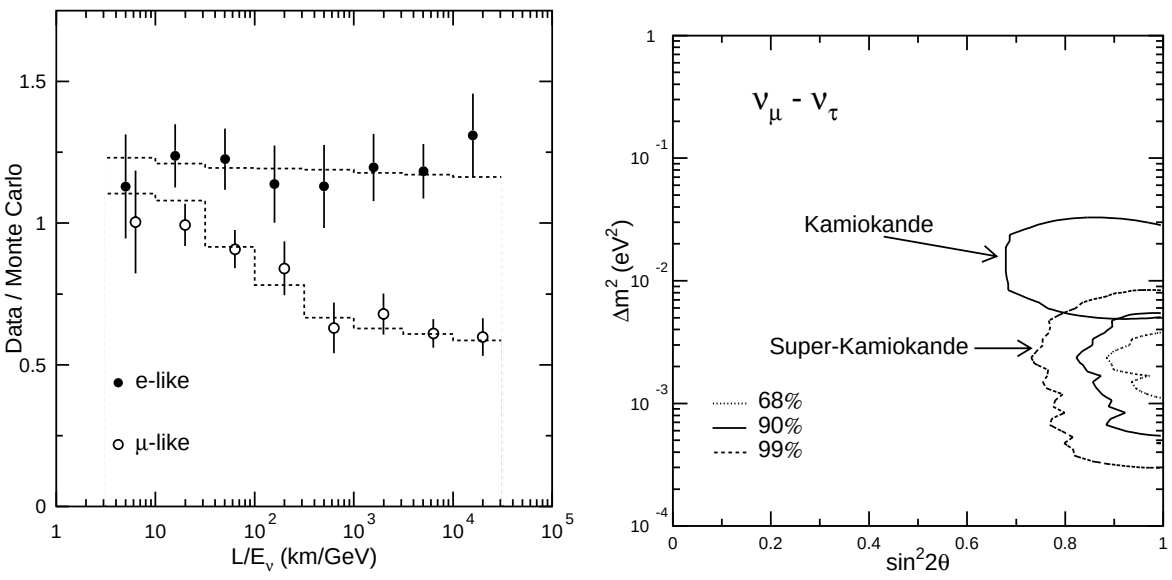

Figure 7: SuperKamiokande data: (a) The ratio of the number of FC events to Monte Carlo events versus reconstructed L/E_ν. The points are the ratios of observed data to MC expectation in the absence of oscillations. The lower dashed line is the expected shape for $\nu_\mu \to \nu_\tau$ for $\Delta m^2 = 2.2 \times 10^{-3}$ and $sin^2 2\theta = 1$. (b) The 68%, 90% and 99% C.L. contours for $sin^2 2\theta$ and Δm^2 for $\nu_\mu \to \nu_\tau$ oscillations. The 90% C.L. contour obtained by the Kamiokande experiment is also shown.

fined to be the energy of an electron that would produce the observed amount of Cherenkov light. $E_{vis} = 1.33\ GeV$ corresponds to $p_\mu \sim 1.4\ GeV/c$.

In a full-detector Monte Carlo simulation, 88% (96%) of sub-GeV e-like (μ-like) events were ν_e (ν_μ) charged-current interactions and 84% (99%) of the multi-GeV e-like (μ-like) events were ν_e (ν_μ) CC interactions. PC events were estimated to be 98% ν_μ charged-current interactions; hence, all the PC events were classified as μ-like, and no single-ring requirement was made.

The zenith angle distributions for e-like and μ-like FC and PC events are shown in Fig. 6. Note the near agreement of the e-like measured events with the MC predictions without oscillations, and instead the deviations from the no oscillation predictions for the μ-like events. Significantly small values of the double ratio $R = (\mu/e)_{data}/(\mu/e)_{MC}$ in both the sub-GeV and multi-GeV samples were obtained. Several sources of systematic uncertainties in these measurement have been considered, but none of these can alter significantly the results. Moreover, the μ-like data exhibit a strong up/down asymmetry in zenith angle (Θ) while no significant asymmetry is observed in the e-like data. The up/down ratio is expected to be near unity, really independent

of the flux model for $E_\nu > 1\ GeV$ (above this value the effects due to the Earth' magnetic field on cosmic rays are small). The experimentally measured up/down ratio is $0.54^{+0.06}_{-0.05} \pm 0.01$ for the multi-GeV FC+PC μ-like events.

SuperKamiokande estimated the oscillation parameters considering the R measurements and the zenith angle shapes separately. The 90% CL allowed regions for each case overlapped at $1 \times 10^{-3} < \Delta m^2 < 4 \times 10^{-3}\ eV^2$ for $sin^2 2\theta = 1$. Fig. 7a shows the ratio of FC data to Monte Carlo for e-like and μ-like events with $p > 400\ MeV/c$ as a function of L/E_ν, compared to the expectation for $\nu_\mu \rightarrow \nu_\tau$ oscillations with the best fit parameters from R versus zenith angle. While the e-like data show no significant variation in L/E_ν, the μ-like events show a significant deficit at large L/E_ν. At large L/E_ν, the ν_μ have presumably undergone numerous oscillations and have averaged out to roughly half the initial rate.

The final values for $\nu_\mu \rightarrow \nu_\tau$ oscillations are $sin^2 2\theta_{\mu\tau} = 1$ and $\Delta m^2 = 0.0022\ eV^2$. The contour plots for the neutrino oscillation parameters for Kamiokande and SuperKamiokande are shown in Fig. 7b. Superkamiokande reported also data on up throughgoing muons, which agree with the predictions with an oscillated flux with the above parameters[15].

7. Conclusions

A wealth of new data on atmospheric neutrinos was presented at the Neutrino'98 Conference. The zenith angle distributions of atmospheric neutrino induced muons differ in shape and in absolute value from the ones predicted in the absence on neutrino oscillations. In the vertical upgoing direction there are about 50% deficits for low and high energy muon events. For ν_e induced electrons there is no strong deviation from prediction. The ratio of muons to electrons normalized to the respective MC predictions enhances the anomaly.

The new data are in agreement with the hypothesis of two flavour $\nu_\mu \rightarrow \nu_\tau$ oscillations, with maximum mixing and $\Delta m^2 \sim 0.0023\ eV^2$; the uncertainty in the Δm^2 is relatively large. The 90% CL contours of MACRO and SuperKamiokande overlap closely.

The present experiments on atmospheric neutrinos are disappearance experiments; it would be nice to have a cross check with an appearance experiment.

One cannot exclude $\nu_\mu \rightarrow \nu_s$ oscillations into a sterile ν_s. Answers to some detailed questions, like the shape of the high energy muon angular distribution may need more data.

We would like to acknowledge the cooperation of many members of the MACRO collaboration, in particular of all the members of the neutrino working group.

8. References

1. J.M. Stone, *Atmospheric neutrinos*, in Proceedings of the 1995 Trieste 4th School on Non-accelerator Particle Astrophysics, Editors E. Bellotti, R.A. Carrigan, G.Giacomelli, N.Paver, World Scientific (1996) p.175. See this paper for early experiments and for the historical development of atmospheric neutrinos studies.
2. G. Barr, T.K. Gaisser and T.Stanev, Phys. Rev. **D39** (1989) 3532.
   M.Honda et al., Phys. Lett. **B248**(1990)193.
   H.Lee and Y.S.Koh, Nuovo Cimento **105B** (1990) 883.
3. L. V. Volkova, Sov. J. Nucl. Phys. **31** (1980) 784.
   K. Mitsui et al., Nuovo Cimento **9C** (1986) 995.
   A.V. Butkevich et al., Sov. J. Nucl. Phys. **50** (1989) 90.
4. Kamiokande Collaboration, K.S. Hirata *et al.*, Phys. Lett. **B205** (1988) 416; Phys. Lett. **B280** (1992) 2; Y. Fukuda *et al.*, Phys. Lett. **B335** (1994) 237; M. Mori *et al.*, Phys. Lett. **B270** (1991) 89.
5. IMB Collaboration, D. Casper *et al.*, Phys. Rev. Lett. **66** (1991) 2561; R. Becker-Szendy *et al.*, Phys. Rev. **D46** (1992) 3720; Phys. Rev. Lett. **69** (1992) 1010.
6. NUSEX Collaboration, M. Aglietta *et al.*, Europhys. Lett. **8** (1989) 611; 23rd ICRC proceedings, Calgary, Canada, Vol. **4** (1993) 446.
7. Frejus Collaboration, Ch. Berger *et al.*, Phys. Lett. **B227** (1989) 489; K. Daum *et al.*, Z. Phys. **C66** (1995) 417.
8. Baksan Collaboration, S. Mikheyev, 5th TAUP Workshop proceedings, Gran Sasso, Italy, 1997.
9. Soudan 2 collaboration, W.W. M. Allison *et al.*, Phys. Lett. **B391** (1997) 491; T. Kafka *Atmospheric Neutrino interactions in Soudan 2*, 5th TAUP Workshop proceedings, Gran Sasso, Italy, 1997.

10. MACRO Collaboration, S. Ahlen *et al.*, Phys. Lett. **B 357**(1995) 481; F.Ronga et al., *Neutrino induced upward going muons with the MACRO detector*, proceedings of Neutrino'96, Helsinki, Finland; P.Bernardini et al., *The measurement of the atmospheric muon flux using MACRO*, INFN/AE-97/21 and Proceedings of the 25th ICRC, Durban, South Africa, vol. 7 (1997) 41.
11. SuperKamiokande collaboration, Y.Fukuda *et al.*, Proceedings of the 1997 Europhysics Conf., Jerusalem, Israel.
12. Soudan 2 Collaboration, B. Peterson, *Contained events and Soudan 2*, invited paper at Neutrino'98, Takayama, Japan; H. Gallagher, *Atmospheric Neutrinos in Soudan 2*, invited paper at the 1998 HEP Conf., Vancouver, Canada.
13. MACRO Collaboration, F. Ronga, *Atmospheric neutrino induced muons in the MACRO detector* invited paper at Neutrino'98, Takayama, Japan; hep-ex/9810008. M.Ambrosio *et al*, Phys. Lett. **B434** (1998) 451; P.Bernardini, *Measurement of the atmospheric neutrino induced muon flux with the MACRO detector*, invited paper at the Vulcano Workshop on Frontier Objects in Astrophysics and Particle Physics, Vulcano, Italy, 25-30 May 1998, hep-ex/9809003.
14. SuperKamiokande Collaboration, T.Kajita, *Results from SuperKamiokande and Kamiokande*, invited paper at Neutrino'98, Takayama, Japan; Y.Fukuda *et al.*, Phys. Rev. Lett. **81** (1998)1562; Phys. Lett. **B433** (1998)9.
15. M.Koshiba, *Kamiokande and SuperKamiokande*, this School.
16. J. Conrad, ν_e *or not* ν_e*? and other neutrino oscillation questions...*, Rapporteur talk at the HEP Conference, Vancouver, Canada (1998).
17. V. Agrawal, T.K. Gaisser, P. Lipari and T. Stanev, Phys.Rev. **D53** (1996) 1314.
18. Morfin, J. G. and Tung W. K., Z. Phys. **C52** (1991) 13.
19. Lohmann W. *et al.*, *Energy loss of muons in the energy range 1-GeV to 10000-GeV.* CERN-EP/85-03 (1985).
20. P. Lipari, M. Lusignoli and F. Sartogo, Phys. Rev. Lett. **74** (1995) 4384.
21. Particle Data Group, R.M. Barnett *et al.* Phys. Rev. **D54** (1996) 375.